# The Open-Chain Trioxide $CF_3OC(O)OOOC(O)OCF_3$

**Stefan von Ahsen,[a] Plácido García,[a] Helge Willner,*[a, c] Maximiliano Burgos Paci,[b] and Gustavo A. Argüello[b]**

**Abstract:** The open-chain trioxide $CF_3OC(O)OOOC(O)OCF_3$ is synthesised by a photochemical reaction of $CF_3C(O)OC(O)CF_3$, CO and $O_2$ under a low-pressure mercury lamp at $-40\,^{\circ}C$. The isolated trioxide is a colourless solid at $-40\,^{\circ}C$ and is characterised by IR, Raman, UV and NMR spectroscopy. The compound is thermally stable up to $-30\,^{\circ}C$ and decomposes with a half-life of 1 min at room temperature. Between $-15$ and $+14\,^{\circ}C$ the activation energy for the dissociation is 86.5 kJ mol$^{-1}$ (20.7 kcal mol$^{-1}$). Quantum chemical calculations have been performed to support the vibrational assignment and to discuss the existence of rotamers.

**Keywords:** fluorine · matrix isolation · photochemistry · trioxides · vibrational spectroscopy

## Introduction

There are many examples in chalcogen chemistry of molecules such as polysulfanes, containing polyelement chains. Single-bonded polyoxy compounds are less common, because their stability decreases as the number of oxygen atoms increases. Some trioxides with bulky organic substituents such as *t*BuOOO-*t*Bu,[1–3] as well as various primary ozonides, have been studied for many years. Khalizov and co-workers reviewed alkyl trioxides recently,[4] but perfluorinated polyoxy compounds are still laboratory curiosities. Only a few perfluoroalkyl trioxides such as $CF_3OOOCF_3$[5–9] and $CF_3OOOC_2F_5$[5, 6] have been isolated and well characterised, whereas the first acyl compound FC(O)OOOC(O)F has been mentioned only in recent years[10] and is still under investigation.[11]

Bis(fluoroformyl) trioxide is formed as a by-product in the synthesis of FC(O)OOC(O)F by the reaction of $F_2/O_2$ mixtures with CO, whereby F atoms act as key species. In a related reaction system, in which $CF_3O$ radicals catalyse the oxidation of CO to $CO_2$,[12, 13] the new peroxide $CF_3OC(O)OOC(O)OCF_3$ was isolated,[13] studied kinetically[14] and characterised structurally.[15] Traces of $CF_3OC(O)OOOC(O)OCF_3$ were detected as a by-product.[13]

Both the peroxide and the trioxide are good thermal sources for $CF_3O$,[16, 17] as is the trioxide for $CF_3OC(O)OO$;[18] both of these radicals are important intermediates in the degradation of CFCs and their replacements.

In this work, we describe improved reaction conditions that lead to a high yield of bis(trifluoromethoxy)trioxodicarbonate ($CF_3OC(O)OOOC(O)OCF_3$) as well as its isolation, spectroscopic characterisation and thermal decay in the presence of excess $N_2$ and CO. Molecular properties are predicted by quantum chemical calculations, which also support the interpretation of the observed spectra.

## Results and Discussion

**Synthetic aspects**: In the reaction mechanism that leads to the known peroxide $CF_3OC(O)OOC(O)OCF_3$,[13] $CF_3O$ radicals generated by the reaction sequence represented by Equations (1) – (3)[13] play a key role. The catalytic oxidation of CO proceeds by the chain reaction given in Equations (4) – (7) and summarised in Equation (8).[12, 13]

$$CF_3C(O)OC(O)CF_3 + h\nu \rightarrow 2\,CF_3 + CO_2 + CO \quad (1)$$

$$2\,CF_3 + 2\,O_2\ (+\ M) \rightarrow 2\,CF_3OO\ (+\ M) \quad (2)$$

$$2\,CF_3OO \rightarrow 2\,CF_3O + O_2 \quad (3)$$

$$2\,CF_3O + 2\,CO\ (+\ M) \rightarrow 2\,CF_3OCO\ (+\ M) \quad (4)$$

[a] Prof. Dr. H. Willner, Dr. S. von Ahsen, P. García
Fakultät 4, Anorganische Chemie
Gerhard-Mercator-Universität Duisburg
Lotharstr. 1, 47048 Duisburg (Germany)
Fax: (+49) 203-379-2231
E-mail: willner@uni-duisburg.de

[b] Dr. M. Burgos Paci, Prof. Dr. G. A. Argüello
INFIQC, Depto. de Físico Química
Facultad de Ciencias Químicas
Universidad Nacional de Córdoba, Ciudad Universitaria
5000 Córdoba (Argentina)
E-mail: gaac@isquim.fcq.unc.edu.ar

[c] Prof. Dr. H. Willner
Present address:
Bergische Universität Wuppertal, FB 9, Anorganische Chemie
Gaussstr. 20, 42097 Wuppertal (Germany)

 **DOI: 10.1002/chem.200304942**  

$$2\,CF_3OCO + 2\,O_2\ (+\ M) \rightarrow 2\,CF_3OC(O)OO\ (+\ M) \quad (5)$$

$$2\,CF_3OC(O)OO \rightarrow 2\,CF_3OCO_2 + O_2 \quad (6)$$

$$2\,CF_3OCO_2 \rightarrow 2\,CF_3O + 2\,CO_2 \quad (7)$$

$$2\,CO + O_2 \rightarrow 2\,CO_2 \quad (8)$$

It was possible to isolate $CF_3OC(O)OOCF_3$[8] and $CF_3OC(O)OOC(O)OCF_3$[13] from the reaction mixture. These compounds were formed by some of the termination reactions [Eqs. (9)–(11)].

$$2\,CF_3OCO_2\ (+\ M) \rightarrow CF_3OC(O)OOC(O)OCF_3 \quad (9)$$

$$CF_3OCO_2 + CF_3O\ (+\ M) \rightarrow CF_3OC(O)OOCF_3 \quad (10)$$

$$CF_3OCO + CF_3OO\ (+\ M) \rightarrow CF_3OC(O)OOCF_3 \quad (11)$$

At a reaction temperature of 0 °C, a thermally labile compound was detected in addition to these products, but it could not be identified clearly, because its IR spectrum was very similar to that of $CF_3OC(O)OOC(O)OCF_3$. The most likely candidate for the unidentified compound was the trioxide $CF_3OC(O)OOOC(O)OCF_3$,[13] which is formed by recombination of the rather long-lived peroxy radical $CF_3OC(O)OO$, formed through Equation (5), with the short-lived $CF_3OCO_2$ radical, generated from Equation (6), in the termination reaction [Eq. (12)].

$$CF_3OCO_2 + CF_3OC(O)OO\ (+\ M) \rightarrow CF_3OC(O)OOOC(O)OCF_3\ (+\ M) \quad (12)$$

At a lower reaction temperature (−40 °C) the trioxide can be obtained as the main product, together with $CO_2$ from the catalytic cycle and the peroxydicarbonate as only a trace. As the primary formation of $CF_3OC(O)OO$ depends on the photolysis rate of trifluoroacetic anhydride (TFAA); its concentration is, in a first approximation, independent of temperature. Nevertheless, the formation of the short-lived species $CF_3OCO_2$ [Eq. (6)] is strongly dependent on $CF_3OC(O)OO$ formation. Therefore, the trioxide $CF_3OC(O)OOOC(O)OCF_3$ is formed according to Equation (12) as the primary product during the synthesis at any temperature.

The reaction given in Equation (9) is responsible for the formation of the peroxide and is important only if the concentration of the short-lived $CF_3OCO_2$ radical is effectively increased. Here the postulated trioxide may act as a reservoir for this radical since, once it is formed, the regeneration of $CF_3OCO_2$ would then be dependent on the reaction temperature as the decay of the trioxide is an activated process [Eq. (13)].

$$CF_3OC(O)OOOC(O)OCF_3 \rightarrow CF_3OC(O)OO + CF_3OCO_2 \quad (13)$$

From Equation (13) together with Equation (6) it follows that the formation of the peroxide $CF_3OC(O)OOC(O)OCF_3$ at higher reaction temperatures (−20 to +10 °C) is only a consequence of the thermal decay of the primarily generated trioxide [Eq. (13)].

We conclude that radical–radical recombination reactions, which usually have no activation barrier and, therefore, no temperature dependence, are not the only ones responsible for the observations. Since unimolecular dissociation of molecules does have an activation barrier, the observed temperature dependence of the reaction system is now rationalised. Moreover, as the dissociation of $CF_3OCO_2$ radicals requires a low activation energy, neither trioxide nor peroxide is formed above room temperature.

Here, trapping of the trioxide at −40 °C, at which it is not only thermally stable but also shows no significant vapour pressure, gives evidence which strongly supports the reaction system discussed above[13] and ensures that it proceeds in the desired direction.

**Spectroscopic properties**: The IR spectrum of pure $CF_3OC(O)OOOC(O)OCF_3$ is very similar to the known IR spectrum of $CF_3OC(O)OOC(O)OCF_3$,[13] since all the characteristic bands appear in the same spectral region. The main differences in the spectra can be found in the $\nu$(C=O), $\nu$(C–O), $\nu$(OO) and $\nu$(OOO) modes. The IR and Raman spectra of $CF_3OC(O)OOOC(O)OCF_3$ are presented in Figure 1.

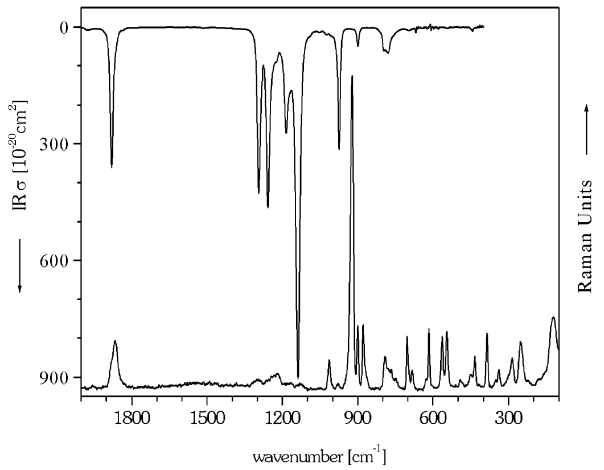


Figure 1. IR (gas-phase) and Raman (solid, −196 °C) spectra of $CF_3OC(O)OOOC(O)OCF_3$.

Table 1 shows an assignment of the observed bands, which are compared with the related peroxide. The assignment is supported by quantum chemical calculations, which are discussed below. Due to the similarity of the masses of all the atoms and comparable bond strengths, all modes except the C=O stretching are strongly mixed. Therefore, the fundamental modes are not described in Table 1.

For $CF_3OC(O)OOOC(O)OCF_3$ only one main absorption band occurs in the carbonyl region (1878 $cm^{-1}$ in both the gas phase and neon matrix), implying that the vibrational coupling of the two $\nu$(C=O) bands is reduced in comparison with $CF_3OC(O)OOC(O)OCF_3$ (where two separate bands at 1887 and 1866 $cm^{-1}$ can be observed). This feature could be interpreted in terms of the elongation and enhanced flexibility of the enlarged oxygen chain. In general, any normal mode in which a movement in the $CF_3OC(O)$ moieties is expected

Table 1. Fundamental modes of $CF_3OC(O)OOOC(O)OCF_3$, compared with $CF_3OC(O)OOC(O)OCF_3$.

| $CF_3OC(O)OOOC(O)OCF_3$ | | | | | | | | | | | | $CF_3OC(O)OOC(O)OCF_3$ | | |
|---|---|---|---|---|---|---|---|---|---|---|---|---|---|---|
| Gas phase | | Ne matrix | Ar matrix | | Raman | | Calcd[a] | | | Assignment | | Gas phase[b] | Ar matrix[b] | Calcd[a] |
| $\nu$ [$cm^{-1}$] | $\sigma$ [$10^{-20}$ $cm^2$] | $\nu$ [$cm^{-1}$] | $\nu$ [$cm^{-1}$] | rel. int.[c] | $\nu$ [$cm^{-1}$] | int. | $\nu$ [$cm^{-1}$] | IR int. [km $mol^{-1}$] | RA int. [amu Å$^4$] | | $C_2$ sym. | $\nu$ [$cm^{-1}$] | $\nu$ [$cm^{-1}$] | $\nu$ [$cm^{-1}$] |
| 1878 | 277 | 1878.3 | 1872 | 41 | 1866 | s | 1935.1 | 67 | 10 | A | $\nu_1$ | 1887 | 1884 | 1940.4 |
| | | | | | | | 1930.9 | 657 | 1.1 | B | $\nu_{24}$ | 1866 | 1857 | 1911.9 |
| 1293 | 549 | 1295.0 | 1291 | 47 | | | 1284.9 | 448 | 0.6 | B | $\nu_{25}$ | 1298 | 1296 | 1286.5 |
| | | | | | | | 1284.6 | 129 | 0.8 | A | $\nu_2$ | | | 1288.1 |
| 1257 | 747 | 1255.3 | 1250 | 60 | | | 1242.7 | 535 | 0.3 | A | $\nu_3$ | 1259 | 1251 | 1242.9 |
| | | | | | | | 1240.9 | 254 | 0.8 | B | $\nu_{26}$ | | | 1242.5 |
| 1185 | 170 | 1185.1 | | | | | 1224.3 | 114 | 3.0 | A | $\nu_4$ | | | 1240.7 |
| | | 1181.8 | 1178 | 34 | | | 1207.4 | 99 | 1.4 | B | $\nu_{27}$ | | 1217.6 | |
| 1170 | 174 | 1165.5 | | | | | 1169.6 | 348 | 2.9 | A | $\nu_5$ | 1195 | 1185 | 1177.2 |
| 1138 | 815 | 1133.6 | 1132 | 100 | | | 1128.0 | 1900 | 1.1 | B | $\nu_{28}$ | 1135 | 1131 | 1118.3 |
| | | 1010.3 | 1009 | 1.7 | 1013 | s | 1025.0 | 34 | 12 | A | $\nu_6$ | 1050 | 1048 | 1069.2 |
| 974 | 230 | 975.6 | 974 | 25 | 976 | vw | 973.0 | 603 | 0.8 | B | $\nu_{29}$ | 989 | 988 | 987.5 |
| | | | | | 923 | vs | 956.3 | 1.1 | 34 | A | $\nu_7$ | | | 958.9 |
| 899 | 35 | 902.2 | 901 | 4.9 | 900 | s | 901.6 | 122 | 1.4 | B | $\nu_{30}$ | 905 | 906 | 905.5 |
| | | | | | 878 | s | 883.2 | 0.55 | 8.1 | A | $\nu_8$ | | | 876.8 |
| 795 | 48 | 792.8 | 790 | 13 | 791 | m | 803.5 | 358 | 5.9 | B | $\nu_{31}$ | – | – | – |
| 789 | 49 | 771.4 | 770 | 5.7 | 778 | w | 775.1 | 32 | 0.1 | B | $\nu_{32}$ | | 756 | 774.4 |
| 778 | 55 | 767.2 | 767 | | 766 | w | 769.5 | 28 | 0.2 | A | $\nu_9$ | | | 774.7 |
| | | 757.8 | 757 | 1.1 | 748 | w | 757.8 | 4.6 | 0.5 | A | $\nu_{10}$ | 744 | 742 | 756.0 |
| | | 751.3 | 749 | | 740 | w | 750.6 | 26 | 0.3 | B | $\nu_{33}$ | | | 746.3 |
| 695 | 10 | 703.2 | 703 | 1.1 | 702 | s | 702.4 | 8.6 | 2.5 | A | $\nu_{11}$ | 669 | 668 | 667.2 |
| | | 684.1 | 682 | 0.18 | 683 | m | 687.0 | 3.4 | 1.1 | B | $\nu_{34}$ | | 727 | 723.3 |
| | | 616.2 | 615 | 0.28 | 616 | s | 608.3 | 1.6 | 1.0 | A | $\nu_{12}$ | 610 | 614 | 607.6 |
| | | | | | | | 608.0 | 1.3 | 1.7 | B | $\nu_{35}$ | | | 606.7 |
| 546 | | 547.0 | 545 | 0.10 | 563 | s | 559.8 | 2.4 | 1.2 | A | $\nu_{13}$ | – | – | – |
| | | | | | | | 555.9 | 0.54 | 2.7 | B | $\nu_{36}$ | | | 556.6 |
| 541 | | 541.9 | 541 | 0.07 | 544 | s | 552.7 | 1.8 | 3.2 | A | $\nu_{14}$ | | 563[d] | 555.6 |
| 442 | | 450.2 | 448 | 0.89 | 449 | | 449.9 | 19 | 1.2 | B | $\nu_{37}$ | 460 | 460 | 460.9 |
| | | | | | 433 | m | 427.4 | 0.21 | 0.5 | B | $\nu_{38}$ | | 431 | 426.1 |
| | | | | | | | 427.2 | 0.16 | 0.8 | A | $\nu_{15}$ | | | 428.5 |
| | | | | | 386 | s | 381.4 | 0.03 | 1.5 | A | $\nu_{16}$ | | 383 | 383.7 |
| | | | | | | | 379.2 | 1.1 | 0.3 | B | $\nu_{39}$ | | | 379.8 |
| | | | | | 339 | w | 329.5 | 0.90 | 0.6 | B | $\nu_{40}$ | | | 327.1 |
| | | | | | 286 | m | 274.3 | 0.29 | 1.3 | A | $\nu_{17}$ | | 343[d] | 340.4 |
| | | | | | 252 | s | 243.4 | 0.50 | 2.9 | A | $\nu_{18}$ | | 242[d] | 231.8 |
| | | | | | 180 | w | 166.1 | 3.6 | 0.1 | B | $\nu_{41}$ | | | 156.0 |
| | | | | | | | 141.3 | 0.08 | 0.1 | B | $\nu_{42}$ | – | – | – |
| | | | | | 121 | s | 116.6 | 0.04 | 0.6 | A | $\nu_{19}$ | | | 161.5 |
| | | | | | | | 100.5 | 0.34 | 0.7 | A | $\nu_{20}$ | | 108[d] | 111.4 |
| | | | | | | | 88.8 | 0.47 | 0.5 | B | $\nu_{43}$ | | | 100.7 |
| | | | | | 72 | s | 70.9 | 0.12 | 0.4 | A | $\nu_{21}$ | | | 74.7 |
| | | | | | | | 57.7 | 0.07 | 0.4 | B | $\nu_{44}$ | | | 56.7 |
| | | | | | | | 29.8 | 0.23 | 0.1 | B | $\nu_{45}$ | | | 33.0 |
| | | | | | | | 27.8 | 0.20 | 0.2 | A | $\nu_{22}$ | | | 39.1 |
| | | | | | | | 21.4 | 0.00 | 0.3 | A | $\nu_{23}$ | | | 26.5 |

[a] B3LYP/6-311G(d,p), this work. [b] From ref. [13]. [c] Relative integrated band intensities. [d] Raman, solid at $-196\,^{\circ}C$.

should give rise to two separate bands in the vibrational spectrum as the movement can be in-phase or off-phase. However, from our spectroscopic resolution (1 $cm^{-1}$ in Ne matrix, 2 $cm^{-1}$ in the gas-phase IR spectra, 4 $cm^{-1}$ in the Raman spectrum), only overlapping bands of the corresponding in-phase and off-phase modes are observed.

$\nu_s$(OOO) is detected as a strong Raman band at 923 $cm^{-1}$. The antisymmetric mode $\nu_a$(OOO) is strongly mixed with the carbon–oxygen stretching modes, as is also calculated for $\nu$(C–O) and $\nu$(OO) in the case of the peroxide $CF_3OC(O)OOC(O)OCF_3$. The $\nu$(OO) fundamentals are useful for distinguishing between the trioxide and peroxide, as the trioxide absorbs at 974 $cm^{-1}$ with moderate intensity while the peroxide has its analogue at 989 $cm^{-1}$ (both gas-phase values).

According to quantum chemical calculations, the most stable isomer of the trioxide is the all-*trans*-sym-$CF_3OC(O)OOOC(O)OCF_3$ (Figure 2) that has $C_2$ symmetry and

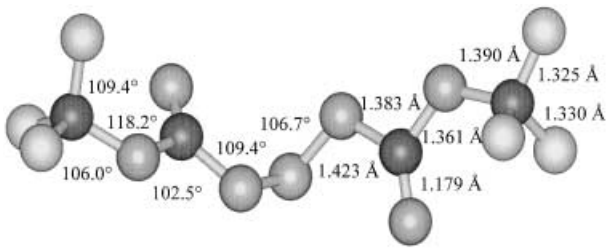


Figure 2. Calculated structure of $CF_3OC(O)OOOC(O)OCF_3$.

  

a *trans* configuration (close to 180°) of all the independent dihedral angles of the 11-atom F-C-O-C-O-O-O-C-O-C-F chain except for the C-O-O-O and O-O-O-C angles, for which $\beta = +90.13°$ (see Figure 2). The irreducible representation of the 45 fundamental vibrations is given in Equation (14) and they can be described approximately by 16 stretching, 19 deformation, two out-of-plane and eight torsion modes.

$$\Gamma_{vib} = 23A\,(\mathrm{IR, Ra\,p}) + 22B\,(\mathrm{IR, Ra\,dp}) \quad (14)$$

The trioxide may exist in 72 possible rotamers: in each $CF_3OC(O)O$ unit three independent dihedral angles can be either 180° or 0°, leading to $2^3 = 8$ species for each unit. If both parts of the molecule are identical, we get eight isomers. If they are different, then $7+6+5+4+3+2+1 = 28$ additional isomers are possible. The two dihedral angles in the COOOC unit, each with a *gauche* configuration, may be symmetric (both 90°) or antisymmetric (90° and −90°), which leads to a total of $2(8+28) = 72$ rotamers. Moreover, the non-symmetric isomers can exist in two enantiomeric forms, which are not counted here.

Full calculations were performed for rotamers that are stable and differ from the most stable form in only a few dihedral angles. Among the possible stable rotamers, the next higher in energy is the *ttc*-sym-*ttt*-$CF_3OC(O)OOOC(O)OCF_3$ rotamer (*cis* configuration of *one* O-C-O-O dihedral, resulting in $C_1$ symmetry) and the energy difference from the most stable isomer is 3.9 kJ mol$^{-1}$. The next is the *ttt*-asy-*ttt*-$CF_3OC(O)OOOC(O)OCF_3$ ($C_1$ symmetry), which is 7.1 kJ mol$^{-1}$ higher in energy than the most stable rotamer. The most important calculated data are presented in Table 2.

The dihedral angles of the most stable all-*trans*-sym-$CF_3OC(O)OOOC(O)OCF_3$ (Figure 2) were calculated to be 179.98°, 179.43° and 177.43° for FCOC, COCO and OCOO, respectively.

For the assignment of the vibrational spectrum, the calculations predict only small differences in the IR spectra for the four most stable rotamers. Irrespective of the state (either gas-phase or solid), the broad bands in the trioxide spectra do not allow a distinction to be made between the different rotamers, so all observed bands can be accounted for by the expected spectrum of the all-*trans*-sym-$CF_3OC(O)OOOC(O)OCF_3$ isomer as described in Table 1. However, in principle, resolution of more fundamental vibrations and discovery of different rotamers should be possible in IR matrix spectra. A rough estimation of the Boltzmann ratio gives percentages of the order of 20 % for the *ttc*-sym-*ttt* and 5 % for the *ttt*-asy-*ttt* rotamer. Since the detection limit of our experimental set-up is in the range of a few per cent (that is, the band intensity of an impurity or trace compound compared with the most intense band of the major species) and since the spectra of the rotamers are very similar, evidence of other isomers was observed, but no proof. Bands at 1863 and 986 cm$^{-1}$ that are also seen in the matrix IR spectrum are in agreement with the calculated data for the *ttc*-sym-*ttt*-$CF_3OC(O)OOOC(O)OCF_3$ isomer in position and expected intensity; a very weak band at 1888 cm$^{-1}$ in the matrix IR spectrum may be due to the all-*trans*-asy-$CF_3OC(O)OOOC(O)OCF_3$ isomer. Nevertheless, all of these bands could also be assigned to an impurity of $CF_3OC(O)OOC(O)OCF_3$, as its IR spectrum differs from that of the trioxide especially at these wavenumbers. Hence, it was not possible to prove *unambiguously* the existence of isomers other than the most stable one, although the appearance of an impurity in the 20 % range is very unlikely according to the NMR analysis.

The UV spectrum of $CF_3OC(O)OOOC(O)OCF_3$ in the 375 – 200 nm region shows an unstructured absorption band

Table 2. Calculations on $CF_3OC(O)OOOC(O)OCF_3$ rotamers [B3LYP/6-311G(d,p)].

| | Rotamer[a] | | | | | | |
|---|---|---|---|---|---|---|---|
| | *ttt*-sym-*ttt* | *ttc*-sym-*ttt* | *ttt*-asy-*ttt* | *ttc*-sym-*ctt* | *tct*-sym-*ttt* | *tct*-sym-*tct* | *ctt*-sym-*ttt* |
| Symmetry | $C_2$ | $C_1$ | $C_1$ | $C_2$ | $C_1$ | $C_2$ | |
| $E$ + ZPC [hartree] | −1278.1804 | −1278.1789 | −1278.1777 | −1278.1775 | −1278.1761 | −1278.1717 | non-existent |
| $\Delta E_{rel}$ [kJ mol$^{-1}$] | 0 | 3.9 | 7.1 | 7.6 | 11.3 | 22.8 | ↓ |
| Ratio[b] | 1 | 0.199 | 0.055 | 0.044 | 0.010 | < 0.001 | *ttt*-sym-*ttt* |
| $\nu$(C=O)[c] | 1935 (67) | 1936 (381) | 1940 (531) | 1919 (227) | 1945 (297) | 1948 (48) | |
| | 1931 (657) | 1914 (412) | 1912 (134) | 1910 (640) | 1933 (458) | 1944 (735) | |
| $\nu$ (stretch) | 1285 (448) | 1289 (282) | 1288 (290) | 1290 (155) | 1286 (322) | 1289 (315) | |
| | 1285 (129) | 1285 (269) | 1281 (274) | 1289 (413) | 1283 (529) | 1279 (961) | |
| | 1243 (535) | 1246 (439) | 1244 (397) | 1248 (519) | 1243 (448) | 1235 (504) | |
| | 1241 (254) | 1243 (401) | 1241 (381) | 1246 (244) | 1230 (372) | 1230 (256) | |
| | 1224 (114) | 1241 (114) | 1230 (183) | 1244 (27) | 1215 (119) | 1204 (574) | |
| | 1207 (99) | 1211 (87) | 1209 (42) | 1229 (119) | 1204 (214) | 1204 (16) | |
| | 1170 (348) | 1164 (376) | 1169 (721) | 1157 (2) | 1160 (941) | 1146 (215) | |
| | 1128 (1900) | 1123 (1847) | 1126 (1493) | 1119 (2471) | 1124 (906) | 1126 (1008) | |
| | 1025 (34) | 1008 (124) | 1031 (85) | 998 (10) | 1014 (110) | 996 (37) | |
| | 973 (603) | 979 (497) | 992 (408) | 983 (323) | 963 (228) | 967 (2) | |
| | 956 (1) | 959 (8) | 965 (79) | 940 (0) | 958 (119) | 954 (313) | |
| | 902 (122) | 896 (34) | 907 (126) | 891 (8) | 893 (55) | 860 (3) | |
| | 83 (1) | 879 (1) | 878 (22) | 872 (0) | 859 (6) | 857 (0) | |
| | 803 (349) | 782 (160) | 829 (171) | 765 (73) | 807 (329) | 808 (351) | |

[a] Nomenclature: $t$ = *trans* (180°), $c$ = *cis* (0°). Labelling order: 1st letter: FCOC dihedral; 2nd letter: COCO dihedral; 3rd letter: OCOO dihedral for first half of molecule, second half the reverse; sym indicates that both central dihedral angles are identical (+90°), asy means one is +90°, and one −90°. Rotamer *ctt*-sym-*ttt* has no energetic minimum; the $CF_3$ unit rotates into the *ttt*-sym-*ttt* structure. [b] Ratio: derived from $\Delta E$ Boltzmann distribution at room temperature (294 K). [c] Wavenumbers [cm$^{-1}$] (intensities [km mol$^{-1}$]).

whose maximum should be below 200 nm. The absorption cross sections could be estimated only approximately, because of the experimental limitations of the matrix technique. Nevertheless, from absorbance measurements at room temperature in the gas phase, the cross sections are probably higher than those obtained from the corresponding peroxide $CF_3OC(O)OOC(O)OCF_3$,[13], showing that the photochemical decomposition of the trioxide can also be important in the above-mentioned reaction scheme including the synthesis of the trioxide or the peroxide.

The $^{19}F$ and $^{13}C$ NMR spectra of $CF_3OC(O)OOOC(O)OCF_3$ show the expected signals and coupling patterns (Table 3).

A more complete characterisation could not be achieved for several experimental reasons: reliable data for melting point, boiling point, vapour pressure and UV cross sections cannot be given as the trioxide $CF_3OC(O)OOOC(O)OCF_3$ is stable only up to about $-30\,^{\circ}C$. At this temperature it is still solid, with a vapour pressure in the 0.1 mbar region. Therefore a structural characterisation of the trioxide in the gas phase was not possible by gas electron diffraction. We were not able to grow crystals by crystallisation of the amorphous solid during several weeks at $-30\,^{\circ}C$.

**Kinetic aspects**: The IR cell, which was maintained at different temperatures between $-15$ and $+14\,^{\circ}C$, was filled with about 1 mbar of pure $CF_3OC(O)OOOC(O)OCF_3$ and then mixed with a large excess of either $N_2$ or CO. Time-spaced spectra were then recorded.

Dissociation in $N_2$ as bath gas gave mainly $CO_2$, $C(O)F_2$, $CF_3OOOCF_3$ and small amounts of $CF_3OC(O)OOC(O)OCF_3$ as products, all of which were identified by their known IR spectra. The rate of trioxide disappearance was measured at $-5$, $-3$, $+8$ and $+14\,^{\circ}C$ (Figure 3). Good straight lines were obtained at any temperature and no pressure dependence was observed.

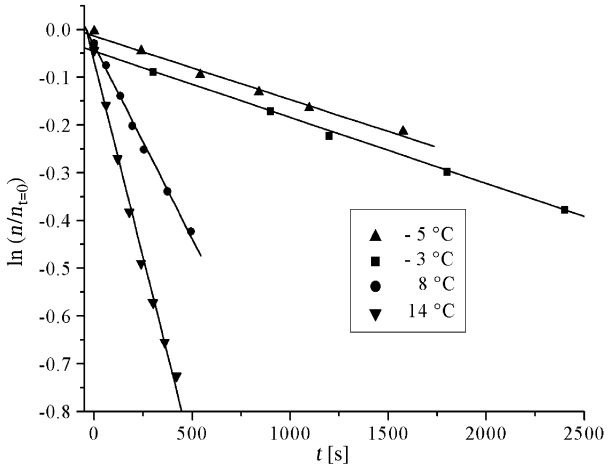


Figure 3. Decay of $CF_3OC(O)OOOC(O)OCF_3$ in the presence of excess $N_2$.

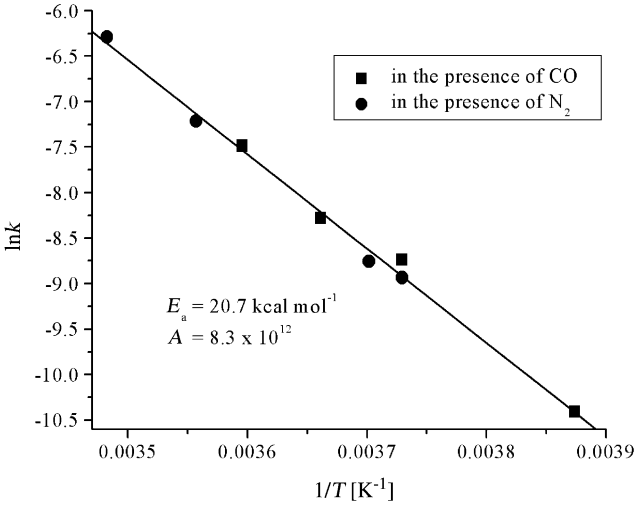


Figure 4. Arrhenius plot of the decay reaction of $CF_3OC(O)OOOC(O)OCF_3$.

Table 3. NMR data for $CF_3OC(O)OOOC(O)OCF_3$ and $CF_3OC(O)OOC(O)OCF_3$.

| Species | $\delta_F$ $CF_3$ [ppm] | $\delta_C$ $CF_3$ [ppm] | $^1J_{CF}$ [Hz] | $\delta_C$ C=O [ppm] |
|---|---|---|---|---|
| $CF_3OC(O)OOOC(O)OCF_3$[a] | −58.5 | +120.0 | 270.3 | +146.2 |
| $CF_3OC(O)OOOC(O)OCF_3$[b] | −61.3 | +119.9 | 268.7 | +145.7 |
| $CF_3OC(O)OOC(O)OCF_3$[b] | −61.3 | +119.9 | 268.7 | +145.5 |

[a] This work: 20 mg substance in 2 mL $CD_2Cl_2$ with a few percent of $CFCl_3$ measured at $-78\,^{\circ}C$, chemical shifts related to $\delta_F CF^{35}Cl_3$ ($-78\,^{\circ}C$) = 0.0 and $\delta_C CD_2Cl_2$ ($-78\,^{\circ}C$) = 54.0, respectively. [b] Ref. [13], $CF_3OC(O)OOC(O)OCF_3$ with $CF_3OC(O)OOOC(O)OCF_3$ as impurity, neat at $-30\,^{\circ}C$, with $CDCl_3/CFCl_3$ mixture as external lock and reference.

Dissociation in the presence of CO gave $CF_3OC(O)C(O)OCF_3$ and $C(O)F_2$ as principal products besides minor quantities of $CF_3OC(O)OOC(O)OCF_3$ and the previously unknown anhydride $CF_3OC(O)OC(O)OCF_3$ (which absorbs strongly at 1056 $cm^{-1}$).[19] In these experiments good straight lines were also obtained at $-15$, $-5$, 0 and $+5\,^{\circ}C$ with similar results to those shown in Figure 3.

As the Arrhenius plot gives the same activation energy within experimental error for both bath gases, we have plotted all the points in Figure 4.

Except for the point at $-5\,^{\circ}C$, there is no superposition of the measured temperatures and good correspondence between the two sets can be observed. This points to a simple unimolecular dissociation mechanism with an energy barrier of 86.5 kJ $mol^{-1}$. Hence the major pathway of the thermal decay of $CF_3OC(O)OOOC(O)OCF_3$ follows Equation (13) and subsequent reactions. The value derived for the activation energy is as expected. It is around 40 kJ $mol^{-1}$ lower than the energy needed to dissociate a typical fluorinated peroxide,[14, 20] and it is also lower than the energy required for the dissociation of $CF_3OOOCF_3$.[21]

The activation energies for hydrogenated dialkyl trioxides, which are all in the range 80–90 kJ $mol^{-1}$, show excellent correspondence with those of other known trioxides.[4] Matrix experiments and quantum chemical calculations also demonstrate that the central oxygen–oxygen bond is the weakest in

  

the trioxides and that the thermal stability decreases in the sequence $CF_3OOOCF_3 > CF_3OC(O)OOOC(O)OCF_3 \approx FC(O)OOOC(O)F \gg FOOOF$, which is demonstrated here by the temperatures required for pyrolysis in matrix experiments (500,[22] 160, 160 °C,[22] for the first three) and by the fact that FOOOF does not exist.[23] Predictions for the bonding energy in fluorinated compounds were made through quantum chemical calculations on the series of symmetrical trioxides ROOOR with $R = CF_3$, FC(O), $CF_3OC(O)$, F, $CH_3$. Some properties of these trioxides were calculated (Table 4).

Table 4. Calculated[a] properties of selected symmetric trioxides ROOOR for the most stable rotamer.

| | $R = CF_3$ | $R = CF_3OC(O)$ | $R = FC(O)$ | $R = F$ | $R = CH_3$ |
|---|---|---|---|---|---|
| $\Delta H_{(O\text{-}O)}$ [kJ mol$^{-1}$][b] | 102.4 | 65.1 | 60.4 | 1.8 | 79.8 |
| $\Delta G_{(O\text{-}O)}$ [kJ mol$^{-1}$] | 47.0 | 8.7 | 6.7 | −50.4 | 25.7 |
| $d$(O–O) [Å] | 1.432 | 1.423 | 1.427 | 1.380 | 1.434 |
| $d$(R–O) [Å] | 1.395 | 1.383 | 1.375 | (1.445) | 1.428 |
| $\alpha$(O-O-O) [°] | 107.4 | 106.7 | 106.6 | 109.7 | 108.0 |
| $q(O_{center})$ [e] | −0.05 | −0.01 | 0.00 | +0.05 | −0.08 |
| $q$ ($O_{side}$) [e] | −0.18 | −0.16 | −0.15 | +0.09 | −0.22 |
| $q$ (C) [e] | +0.70 | +0.54 | +0.56 | | −0.09 |

[a] B3LYP/6–311G(d,p). [b] Can be seen as an activation barrier of the unimolecular decomposition of ROOOR into RO$^\bullet$ + ROO$^\bullet$.

Why does the fluorinated compound $CF_3OC(O)OOOC(O)OCF_3$ behave (in the case of its activation barrier) more like a hydrocarbon trioxide (for example, $CH_3OOOCH_3$), and why does $CF_3OOOCF_3$ differ so greatly from ROOOR when $R = FC(O)$ and $CF_3OC(O)$? A reasonable explanation lies in the interaction between two effects that dominate the stability of the trioxy bridge.

From the calculated values of charges on the OOO chain in Table 4, it may be concluded that an optimum of accumulated charge exists: the decreasing negative charge when going from $CH_3OOOCH_3$ to $CF_3OOOCF_3$ leads to a strong stabilisation of the molecule. The extremely electronegative fluorine in the hypothetic molecule FOOOF even induces a positive charge on the oxygen atoms that destabilises the molecule.

A carbonyl moiety bonded to the trioxy group destabilises the trioxide chain and favours dissociation, as a resonance-stabilised carboxy radical is formed. Hence, an asymmetric trioxide will always dissociate according to Equation (15) and the trioxides ROOOR with $R = FC(O)$, $CF_3OC(O)$ are less stable than $CH_3OOOCH_3$ and $CF_3OOOCF_3$.

$$ROOOC(O)R' \rightarrow ROO + R'CO_2 \quad (15)$$

Since a $CF_3O$ group behaves like a "pseudo-fluorine atom",[17] shown here by comparing $CF_3OC(O)OOOC(O)OCF_3$ with $FC(O)OOOC(O)F$[11] and also discussed in studies of the pairs $CF_3OCO$[17]/FCO[24] and $CF_3OC(O)OOC(O)OCF_3$[13]/$FC(O)OOC(O)F$,[25] some still-unknown properties of the species may be foreseen: the hypothetical tetroxide $CF_3OOOOCF_3$ would probably be stable at liquid-nitrogen temperature but would dissociate above this temperature into $CF_3OOO$ and $CF_3O$, in analogy to FOOF, which decays into F and FOO; however, the pentoxide $CF_3O_5CF_3$ should not exist, in accordance with the non-existent FOOOF.[23]

## Experimental Section

*The polyoxides $CF_3OC(O)OOOC(O)OCF_3$ and $CF_3OC(O)OOC(O)OCF_3$ are potentially explosive, especially in the presence of oxidisable materials. All reactions should be carried out in millimolar quantities only and it is important to take safety precautions, especially when these compounds are handled in the liquid or solid state.*

**Synthesis**: Volatile materials were manipulated in glass vacuum lines, which were equipped with two capacitance pressure gauges (221 AHS 1000 and 221 AHS 10; MKS Baratron, Burlington, MA), three U-traps used for trap-to-trap condensation, and valves with PTFE stems. The vacuum line was connected to an IR gas cell (20 cm optical path length, Si windows) inside the sample chamber of an FTIR spectrometer (Impact 400 D; Nicolet, Madison, WI). This enabled us to observe the course of reactions and the purification process.

The synthesis of $CF_3OC(O)OOOC(O)OCF_3$ was a modification of the published procedure for the generation of $CF_3OC(O)OOC(O)OCF_3$[13] at lower temperature. A Pyrex glass photoreactor (5 L) equipped with a water-cooled mercury low-pressure lamp (15 W, TK15; Hereaus, Hanau, Germany) in a quartz inlet was connected to a vacuum line. In a typical experiment trifluoroacetic acid anhydride (5 mbar, 1.0 mmol, 99 %; Merck, Darmstadt, Germany) was placed in the reactor together with carbon monoxide (150 mbar, 31 mmol, 99 %; Messer Griesheim, Krefeld, Germany) and oxygen (300 mbar, 62 mmol, 99 %; Messer Griesheim, Krefeld, Germany). The reactor was cooled to −40 °C in an ethanol bath cooled with a cryostat (Lauda-Wobser GmbH, Lauda, Germany). After about 2 h of illumination with the mercury lamp, when the CO was nearly consumed, more CO (150 mbar) was added to the reactor. After 5 h most of the TFAA had reacted. The reaction gas passed the three U-traps in the vacuum line, cooled with liquid nitrogen, while the reactor was allowed to reach room temperature slowly. Then the products were gathered in one trap and fractionated by warming this trap to −40 °C, while the volatile material passed the other traps held at −90 °C and −196 °C. Pure solid trioxide $CF_3OC(O)OOOC(O)OCF_3$ was left in the −40 °C trap. Small amounts of the peroxide $CF_3OC(O)OOC(O)OCF_3$ could, if present, be separated from the product by pumping it off at −37 °C.

**Preparation of the matrices**: A small amount of $CF_3OC(O)OOOC(O)OCF_3$ (approximately 0.05 mmol) was transferred into a small U-trap, which was mounted on a quartz pyrolysis nozzle placed directly in front of the matrix support held at 16 K for Ar or 7 K for Ne. The matrix gas Ne or Ar was directed over the $CF_3OC(O)OOOC(O)OCF_3$ sample held at −85 °C by means of an ethanol bath. For each matrix experiment 1–3 mmol Ne or Ar was used, passing the trap within 20–60 min. To study the thermal stability of the trioxide, the pyrolysis nozzle was heated to 160 °C. Details of the matrix apparatus are given elsewhere.[26]

**Kinetic measurements**: The kinetic measurements were performed in a double-walled IR gas cell placed in the sample compartment of an IR spectrometer. The cell was maintained at different temperatures between −15 and +14 °C. Small samples (approximately 1 mbar) of pure $CF_3OC(O)OOOC(O)OCF_3$ were fed into the cell from the storage vessel and subsequently mixed with $N_2$ (99.99 %; La Oxígena, Argentina) or CO (99.9 %; Praxair, Argentina) up to 550 mbar total pressure. Then time-spaced spectra were recorded.

The disappearance of $CF_3OC(O)OOOC(O)OCF_3$ was measured using the bands at 1879 and 973 cm$^{-1}$. At these wavenumbers the products do not absorb. For the analysis of most of the products observed ($CO_2$, $CF_3OOOCF_3$, $CF_2O$, $CF_3OC(O)OOC(O)OCF_3$), calibrated reference spectra from pure samples were recorded.

**Instrumentation**: Gas and matrix IR spectra were recorded on an IFS 28 FTIR or an IFS 66 v/S FTIR spectrometer (Bruker, Karlsruhe, Germany) with resolutions of 2 cm$^{-1}$ (gas phase) or 1 cm$^{-1}$ (matrix) in the range 5000–400 cm$^{-1}$ with DTGS detectors in combination with KBr beam splitters; 64 scans were co-added for each spectrum.

Raman spectra were recorded with an RFS 100/S FT Raman spectrometer (Bruker, Karlsruhe, Germany) with a resolution of 4 cm$^{-1}$. The sample was

condensed under high vacuum on a copper finger cooled with liquid nitrogen and excited by a 500 mW Nd YAG laser (DPY 301; ADLAS, Lübeck, Germany).

UV spectra were recorded with a Perkin–Elmer Lambda 900 UV/Vis spectrometer (Perkin–Elmer, Norwalk, CT) with a resolution of 1 nm and using quartz optics for both matrix-isolated and gas-phase samples. For the latter a 10.5 cm optical pathlength, a 100 mL gas cell was used.

**Calculations**: All calculations were performed with the Gaussian 98 software package[27] with density functional theory (DFT).[28] The molecular geometries were first optimised to standard convergence criteria by the DFT hybrid method with Becke's nonlocal three-parameter exchange,[29, 30] the Lee, Yang and Parr correction[31] (B3LYP), and a 6-311G(d,p) basis set. Then harmonic vibrational wavenumbers were calculated using the optimised structure and an identical basis set and method. The calculation of the most stable rotamers started with the (most stable) all-*trans*-sym-$CF_3OC(O)OOOC(O)OCF_3$ and included only rotamers with few changes in the molecule geometry, as other isomers show strongly increasing energy. Relative energies of the rotamers (Table 2) and O–O bond energies of different trioxides (Table 4) were evaluated for standard conditions.

**Nomenclature**: *E/Z* nomenclature can be used, as well as *cis/trans*, to determine the configuration of substituents at a bond. Usually this is found to describe the connectivity around a double bond. The use of *syn(-planar)/anti(-periplanar)* as part of the molecule name yields correct labelling of the rotamer. In order to follow the nomenclature of related radicals such as $CF_3OC(O)OO$[18] (where the bond order in the peroxy unit is between 1 and 2, allowing the use of *cis/trans*) and to point out the importance of the *transoid* configuration of the molecular chain, the *cis/trans* nomenclature is preferred here. As the two dihedral angles in the COOOC bridge are in any case around 90° (*gauche* configuration) the differentiation between $+90°$, $+90°$ or $+90°$, $-90°$ is given by the prefix sym or asy (for symmetric or antisymmetric), respectively.

## Acknowledgement

Financial support by the Deutsche Forschungsgemeinschaft (DFG) as well as a grant for the interchange of scientists supported jointly by DAAD (Germany) and ANPCyT (Argentina) through the PROALAR program are gratefully acknowledged.

[1] P. D. Bartlett, G. Guaraldi, *J. Am. Chem. Soc.* **1966**, *89*, 4799.
[2] J. E. Bennett, G. Brunton, R. Summers, *J. Chem. Soc. Perkin Trans. 2* **1980**, 981.
[3] A. F. Khalizov, O. N. Makarova, S. L. Khursan, V. V. Shereshovets, *React. Kinet. Catal. Lett.* **1995**, *54*, 427.
[4] A. F. Khalizov, S. L. Khursan, V. V. Shereshovets, *Kinet. Catal.* **1999**, *40*, 194.
[5] L. R. Anderson, W. B. Fox, *J. Am. Chem. Soc.* **1967**, *89*, 4313.
[6] J. Thompson, *J. Am. Chem. Soc.* **1967**, *89*, 4316.
[7] D. D. Desmarteau, *Inorg. Chem.* **1970**, *9*, 2179.
[8] F. A. Hohorst, D. D. Desmarteau, L. R. Anderson, D. E. Gould, W. B. Fox, *J. Am. Chem. Soc.* **1973**, *95*, 3866.
[9] K. I. Gobbato, M. F. Klapdor, D. Mootz, W. Poll, S. E. Ulic, H. Willner, H. Oberhammer, *Angew. Chem.* **1995**, *107*, 2433; *Angew. Chem. Int. Ed. Engl.* **1995**, *34*, 2244.
[10] G. Bednarek, G. A. Argüello, R. Zellner, *Ber. Bunsenges. Phys. Chem.* **1996**, *100*, 445.
[11] H. Pernice, M. Berkei, H. Willner, G. Henkel, M. L. McKee, T. R. Webb, G. A. Argüello, unpublished results.
[12] F. E. Malanca, G. A. Argüello, E. H. Staricco, R. P. Wayne, *J. Phys. Chem. A* **1998**, *117*, 163.
[13] G. A. Argüello, H. Willner, F. E. Malanca, *Inorg. Chem.* **2000**, *39*, 1195.
[14] M. A. Burgos, P. Garcia, G. A. Argüello, H. Willner, *Int. J. Chem. Kinet.* **2003**, *35*, 15.
[15] D. Hnyk, J. Machácek, G. A. Argüello, H. Willner, H. Oberhammer, *J. Phys. Chem. A* **2003**.
[16] G. A. Argüello, H. Willner, *J. Phys. Chem. A* **2001**, *105*, 3466.
[17] S. von Ahsen, J. Hufen, H. Willner, J. S. Francisco, *Chem. Eur. J.* **2002**, *8*, 1189.
[18] S. von Ahsen, H. Willner, J. S. Francisco, *Chem. Eur. J.* **2002**, *8*, 4675.
[19] P. Garcia, H. Willner, M. A. Burgos, G. A. Argüello, unpublished results.
[20] H. Sawada, *Chem. Rev.* **1996**, *96*, 1779.
[21] J. Czarnowski, H. J. Schumacher, *Int. J. Chem. Kinet.* **1981**, *13*, 639.
[22] S. Sander, H. Pernice, H. Willner, *Chem. Eur. J.* **2000**, *6*, 3645.
[23] M. W. Chase, *J. Phys. Chem. Ref. Data* **1996**, *25*, 551.
[24] D. E. Milligan, M. E. Jacox, A. M. Bass, J. J. Comeford, D. E. Mann, *J. Chem. Phys.* **1965**, *42*, 3187.
[25] A. J. Arvía, P. J. Aymonino, H. J. Schumacher, *Angew. Chem.* **1960**, *72*, 327.
[26] G. A. Argüello, H. Grothe, M. Kronberg, H. Willner, H. G. Mack, *J. Phys. Chem.* **1995**, *99*, 17525.
[27] Gaussian 98 (Revision A.5), M. J. Frisch, G. W. Trucks, H. B. Schlegel, G. E. Scuseria, M. A. Robb, J. R. Cheeseman, V. G. Zakrzewski, J. A. Montgomery, R. E. Stratmann, J. C. Burant, S. Dapprich, J. M. Millam, A. D. Daniels, K. N. Kudin, M. C. Strain, O. Farkas, J. Tomasi, V. Barone, M. Cossi, R. Cammi, B. Mennucci, C. Pomelli, C. Adamo, S. Clifford, J. Ochterski, G. A. Petersson, P. Y. Ayala, Q. Cui, K. Morokuma, D. K. Malick, A. D. Rabuck, K. Raghavachari, J. B. Foresman, J. Cioslowski, J. V. Ortiz, B. B. Stefanov, G. Liu, A. Liashenko, P. Piskorz, I. Komaromi, R. Gomperts, R. L. Martin, D. J. Fox, T. Keith, M. A. Al-Laham, C. Y. Peng, A. Nanayakkara, C. Gonzalez, M. Challacombe, P. M. W. Gill, B. G. Johnson, W. Chen, M. W. Wong, J. L. Andres, M. Head-Gordon, E. S. Replogle, J. A. Pople, Gaussian, Inc., Pittsburgh, PA, **1998**.
[28] W. Kohn, L. J. Sham, *Phys. Rev. A* **1965**, *140*, 1133.
[29] A. D. Becke, *J. Chem. Phys.* **1993**, *98*, 1372.
[30] A. D. Becke, *J. Chem. Phys.* **1993**, *98*, 5648.
[31] C. Lee, W. Yang, R. G. Parr, *Phys. Rev. B* **1988**, *41*, 785.

Received: March 13, 2003 [F4942]

  